Article

Making Amines Strong Bases: Thermodynamic Stabilization of Protonated Guests in a Highly-Charged Supramolecular Host

Michael D. Pluth, Robert G. Bergman, and Kenneth N. Raymond

J. Am. Chem. Soc., **2007**, 129 (37), 11459-11467• DOI: 10.1021/ja072654e • Publication Date (Web): 22 August 2007

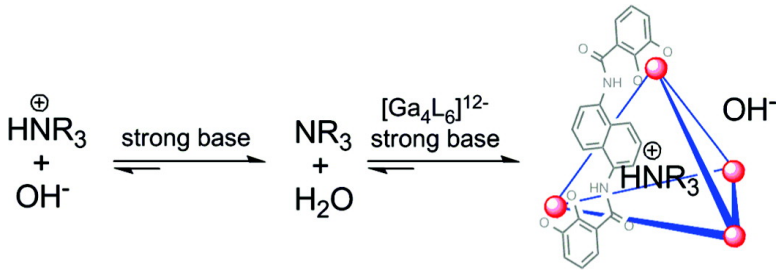

More About This Article

Additional resources and features associated with this article are available within the HTML version:

- Supporting Information
- Links to the 31 articles that cite this article, as of the time of this article download
- Access to high resolution figures
- Links to articles and content related to this article
- Copyright permission to reproduce figures and/or text from this article

View the Full Text HTML

J|A|C|S
ARTICLES
Published on Web 08/22/2007

Making Amines Strong Bases: Thermodynamic Stabilization of Protonated Guests in a Highly-Charged Supramolecular Host[1]

Michael D. Pluth, Robert G. Bergman,* and Kenneth N. Raymond*

Contribution from the Department of Chemistry, University of California, Berkeley, California, 94720-1460

Received April 24, 2007; E-mail: rbergman@berkeley.edu; raymond@socrates.berkeley.edu

Abstract: A highly charged, cavity-containing supramolecular assembly formed by metal−ligand interactions acts as a host to dramatically shift the effective basicity of encapsulated protonated amine guests. The scope of encapsulated protonated amine and phosphine guests shows size selectivity consistent with a constrained binding environment. Protonation of the encapsulated guests is confirmed by ^{31}P NMR studies, mass spectrometry studies, and the pH dependence of guest encapsulation. Rates of guest self-exchange were measured using the selective inversion recovery method and were found to correlate with the size rather than with the basicity of the guests. The activation parameters for guest self-exchange are consistent with the established mechanism for guest exchange. The binding constants of the protonated amines are then used to calculate the effective basicity of the encapsulated amines. Depending on the nature of the guest, shifts in the effective basicities of the encapsulated amines of up to 4.5 pK_a units are observed, signifying a substantial stabilization of the protonated form of the guest molecule and effectively making phosphines and amines strong bases.

Introduction

Drawing inspiration from Nature, synthetic chemists have admired and now emulate the highly specialized ability of enzymes to catalyze chemical reactions using a variety of forces to activate otherwise unreactive substrates. Such enhanced reactivities in the confines of enzyme active sites have driven chemists to try to both explain and duplicate these levels of selectivity in the laboratory, often by using synthetic host molecules with well-defined interior cavities. Lehn, Cram, Pedersen, and Breslow pioneered the study of synthetic molecular hosts through the investigation of crown ethers and cryptands.[2−4] Much like enzymes, the chemical environment of such assemblies—defined by the size, shape, charge, and functional group availability—in a synthetic host can greatly influence the guest-binding characteristics. Since the initial reports of guest binding by synthetic supramolecular assemblies, the complexity of structures and reactivities of host−guest systems have increased dramatically. While this increased complexity allows for the tuning of host−guest properties, the synthetic demands required to produce these often elaborate structures can be daunting. Several groups have circumvented this problem by exploiting the self-assembly process, by which complex supramolecular architectures can be made from relatively simple subunits.

Nature has used enzymes to activate otherwise unreactive compounds in remarkable ways. For example, DNases are capable of hydrolyzing phosphate diester bonds in DNA within seconds,[5−7] whereas under the same conditions, in the absence of enzyme, this hydrolysis has an estimated half-life of 200 million years.[8] A common motif used by Nature to activate unreactive substrates is the precise arrangement of hydrogen-bonding networks and electrostatic interactions between the bound substrate and adjacent residues of the protein.[9] Well-tuned pK_a-matching[10] from the precise arrangement of hydrogen bond donors and acceptors can generate pK_a shifts of over 8 pK_a units, as shown in bacteriorhodopsin.[11] Similarly, purely electrostatic interactions can greatly favor charged states and have been responsible for pK_a shifts of up to 5 pK_a units for acetoacetate decarboxylase.[12]

A number of reports in the literature have documented synthetic chemists' approaches to mimicking such pK_a shifts using cyclodextrins and cucurbiturils as synthetic host molecules which are able to preferentially bind a guest in a specific charge state.[13−16] Recent work by Nau and co-workers has

(1) Paper number 36 in the series Coordination Number Incommensurate Cluster Formation. For the previous paper in the series, see: Tiedemann, B.E.F.; Raymond, K. N. *Angew. Chem., Int. Ed.* **2007**, *119*, 5064−5066.
(2) Cram, D. J. *Angew. Chem., Int. Ed.* **1988**, *27*, 1009−1020.
(3) Lehn, J.-M. *Angew. Chem., Int. Ed.* **1988**, *27*, 89−112.
(4) Breslow, R.; Dong, S. D. *Chem. Rev.* **1998**, *98*, 1997−2011.
(5) Chin, J. *Acc. Chem. Res.* **1991**, *24*, 145−152.
(6) Uhlenbeck, O. C. *Nature* **1987**, *328*, 596−600.
(7) Zoug, A. J.; Michael, D. B.; Cech, T. R. *Nature* **1986**, *324*, 429.
(8) Chin, J.; Banaszczyk, M. *J. Am. Chem. Soc.* **1989**, *111*, 4103−4105.
(9) Ha, N.-C.; Kim, M.-S.; Lee, W.; Choi, K. Y.; Oh, B.-H. *J. Biol. Chem.* **2000**, *275*, 41100−41106.
(10) Cleland, W. W.; Frey, P. A.; Cerlt, J. A. *J. Biol. Chem.* **1998**, *273*, 25529−25532.
(11) Szaraz, S.; Oesterhelt, D.; Ormos, P. *Biophys. J.* **1994**, *67*, 1706−1712.
(12) Westheimer, F. H. *Tetrahedron* **1995**, *51*, 3−20.
(13) Marquez, C.; Nau, W. M. *Angew. Chem., Int. Ed.* **2001**, *40*, 3155−3160.
(14) Mohanty, J.; Bhasikuttan, A. C.; Nau, W. M.; Pal, H, *J. Phys. Chem. B* **2006**, *110*, 5132−5138.

10.1021/ja072654e CCC: $37.00

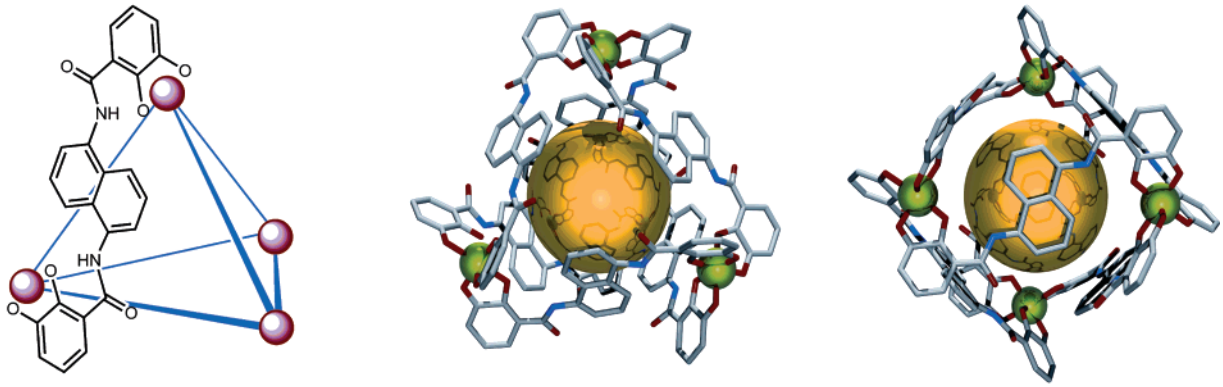

Figure 1. (Left) Schematic representation of **1** with one ligand is shown for clarity. (Middle) Model of **1** with a generic spherical guest viewed down the aperture on the three-fold axis through which guests exchange. (Right) Model of **1** with a generic spherical guest viewed down the two-fold axis.

documented solution-state pK_a shifts of 2 pK_a units that greatly favor the charged species of protonated amines and diazo compounds. Similar studies using substituted calix[4]arenes have used host-induced pK_a shifts to impact fluorescence quenching for the detection of citrate over other inorganic ions such as acetate or tartrate.[17] Such synthetic assemblies have relied on hydrogen-bonding or ion−dipole interactions. Similarly, a number of studies have investigated the effects of charge on binding affinities in supramolecular host−guest systems.[18,19] Many computational studies have investigated the extent of purely electrostatic interactions in such pK_a shifts, but designing experiments to separate the electrostatic contributions from other forces remains difficult. We previously reported the use of a metal−ligand assembly to thermodynamically stabilize protonated guests and exploited this stabilization to catalyze the hydrolysis of acid-labile orthoformates.[20] Herein, we expand on our initial report and provide the substrate scope, guest-exchange dynamics, and thermodynamic stabilities for protonated amines.

Results and Discussion

Binding of Protonated Guests. During the past decade, the Raymond group has developed supramolecular assemblies of the stoichiometry M_4L_6 (M = Ga^{III} (**1**), Al^{III}, In^{III}, Fe^{III}, Ti^{IV}, or Ge^{IV}, L = *N*,*N*′-*bis*(2,3-dihydroxybenzoyl)-1,5-diaminonaphthalene) (Figure 1).[21−24] The metal−ligand interactions in these structures form a well-defined self-assembled tetrahedron with the ligands spanning each edge and the metal ions occupying the vertices. The *tris*-bidentate coordination at the metal vertices makes each vertex a stereocenter, and the strong mechanical coupling of the ligands transfers the chirality of one metal vertex to the others, thereby forming the ΔΔΔΔ or ΛΛΛΛ configurations of the assembly.[25,26] While the 12− overall charge imparts water solubility, the naphthalene walls of the assembly provide a hydrophobic environment which is isolated from the bulk aqueous solution. A wide variety of small monocationic guests ranging from simple organic cations to organometallic catalysts have been encapsulated in **1**. The mechanism of guest exchange has been studied, and it has been shown that the apertures along the three-fold axis of **1** allow for guest ingress and egress.[27,28] Both stoichiometric[29,30] and catalytic[31] reactions have been carried out inside **1** using the constrained environment with size- and stereo-selectivity. Furthermore, **1** itself has been used as a catalyst for the sigmatropic rearrangement of enammonium cations[32,33] and the hydrolysis of acid-labile orthoformates.[20] Making use of the hydrophobicity and polyanionic charge of **1**, a number of highly reactive cations have been kinetically stabilized by encapsulation. These include tropylium,[34] iminium ions,[35] diazonium salts,[36] and reactive phosphonium species,[34,37] all of which decompose rapidly in water and in the absence of **1** are stable only under anhydrous or extremely acidic aqueous conditions.

The ability of **1** to encapsulate monocations and to stabilize species that are normally stable only under acidic aqueous conditions prompted our investigation of protonated molecules as guests. The addition of basic amines, such as TMEDA (*N*,*N*,*N*′,*N*′-tetramethyl-1,2-diaminoethane), to **1** revealed upfield ^{1}H NMR resonances corresponding to the encapsulated guest (Figure 2). Further evidence for encapsulation is observed from

(15) Zhang, X.; Gramlich, G.; Wang, X.; Nau, W. M. *J. Am. Chem. Soc.* **2002**, *124*, 254−263.
(16) Bakirci, H.; Koner, A. L.; Schwarzlose, T.; Nau, W. M. *Chem. Eur. J.* **2006**, *12*, 4799−4807.
(17) Koner, A. L.; Schatz, J.; Nau, W. M.; Pischel, U. *J. Org. Chem.* **2007**, *72*, 3889−3895.
(18) Haas, C. H.; Biros, S. M.; Rebek, J., Jr. *J. Chem. Soc., Chem. Commun.* **2005**, *48*, 6044−6045.
(19) Shinkai, S.; Araki, K.; Manabe, O. *J. Chem. Soc., Chem. Commun.* **1988**, *3*, 187−189.
(20) Pluth, M. D.; Bergman, R. G.; Raymond, K. N. *Science* **2007**, *316*, 85−88.
(21) Caulder, D. L.; Bruckner, C.; Powers, R. E.; Konig, S.; Parac, T. N.; Leary, J. A.; Raymond, K. N. *J. Am. Chem. Soc.* **2001**, *123*, 8923−8938.
(22) Caulder, D. L.; Powers, R. E.; Parac, T. N.; Raymond, K. N. *Angew. Chem., Int. Ed.* **1998**, *37*, 1840−1843.
(23) Caulder, D. L.; Raymond, K. N. *J. Chem. Soc., Dalton Trans. Inorg. Chem.* **1999**, *8*, 1185−1200.
(24) Caulder, D. L.; Raymond, K. N. *Acc. Chem. Res.* **1999**, *32*, 975−982.
(25) Terpin, A. J.; Ziegler, M.; Johnson, D. W.; Raymond, K. N. *Angew. Chem., Int. Ed.* **2001**, *40*, 157−160.
(26) Ziegler, M.; Davis, A. V.; Johnson, D. W.; Raymond, K. N. *Angew. Chem., Int. Ed.* **2003**, *42*, 665−668.
(27) Davis, A. V.; Fiedler, D.; Seeber, G.; Zahl, A.; van Eldik, R.; Raymond, K. N. *J. Am. Chem. Soc.* **2006**, *128*, 1324−1333.
(28) Davis, A. V.; Raymond, K. N. *J. Am. Chem. Soc.* **2005**, *127*, 7912−7919.
(29) Leung, D. H.; Bergman, R. G.; Raymond, K. N. *J. Am. Chem. Soc.* **2006**, *128*, 9781−9797.
(30) Leung, D. H.; Fiedler, D.; Bergman, R. G.; Raymond, K. N. *Angew. Chem., Int. Ed.* **2004**, *43*, 963−966.
(31) Leung, D. H.; Bergman, R. G.; Raymond, K. N. *J. Am. Chem. Soc.* **2007**, *129*, 2746−2747.
(32) Fiedler, D.; Bergman, R. G.; Raymond, K. N. *Angew. Chem., Int. Ed.* **2006**, *45*, 745−748.
(33) Fiedler, D.; van Halbeek, H.; Bergman, R. G.; Raymond, K. N. *J. Am. Chem. Soc.* **2006**, *128*, 10240−10252.
(34) Brumaghim, J. L.; Michels, M.; Pagliero, D.; Raymond, K. N. *Eur. J. Org. Chem.* **2004**, *24*, 5115−5118.
(35) Dong, V. M.; Fiedler, D.; Carl, B.; Bergman, R. G.; Raymond, K. N. *J. Am. Chem. Soc.* **2006**, *128*, 14464−14465.
(36) Brumaghim, J. L.; Michels, M.; Raymond, K. N. *Eur. J. Org. Chem.* **2004**, *22*, 4552−4559.
(37) Ziegler, M.; Brumaghim, J. L.; Raymond, K. N. *Angew. Chem., Int. Ed.* **2000**, *39*, 4119−4121.

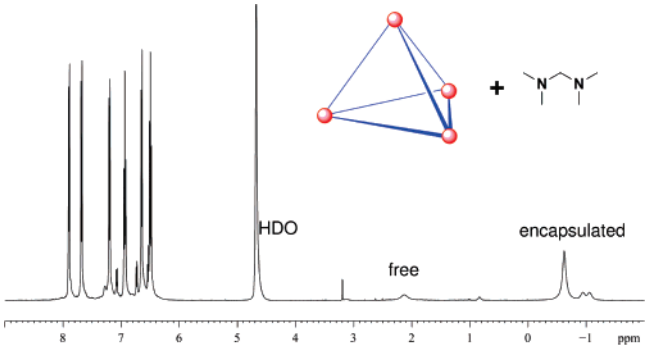

Figure 2. ^{1}H NMR spectrum [H^{+}-TMEDA ⊂ **1**]$^{11-}$ in D_2O (25 °C, 11 mM, 500 MHz).

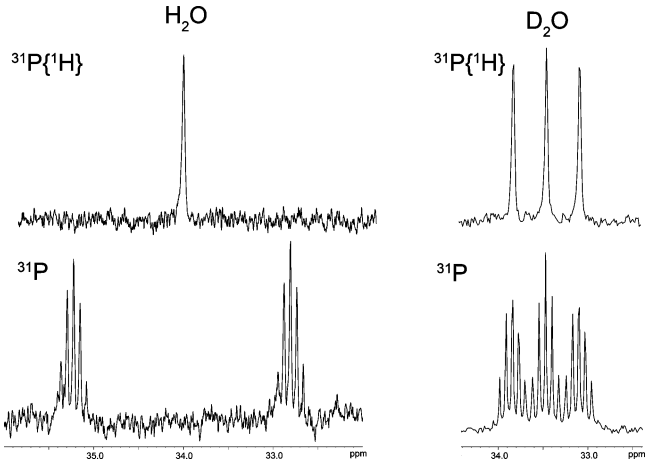

Figure 3. (Left) ^{31}P{^{1}H} (top) and ^{31}P (bottom) NMR spectra of [H^{+}-DMPM ⊂ **1**]$^{11-}$ in H_2O. (Right) ^{31}P{^{1}H} (top) and ^{31}P (bottom) NMR spectra of [H^{+}-DMPM ⊂ **1**]$^{11-}$ in D_2O.

a 2D ^{1}H NOESY spectrum, which clearly shows strong through-space correlation between the naphthalene protons of the assembly and the encapsulated guest. Treatment of $Na_{12}[Ga_4L_6]$ with TMEDA showed only a singlet at 1.0 ppm in the ^{23}Na NMR spectrum corresponding to free solvated sodium ions, suggesting that a Na−TMEDA adduct is not the encapsulated guest.

In order to determine whether protonated or neutral bases were encapsulated in **1**, an analogous phosphine, DMPM (*bis*(dimethylphosphino)methane) was added to **1** for observation of the guest by ^{31}P NMR. As in the case for TMEDA, new upfield resonances corresponding to encapsulated DMPM were observed both in the ^{1}H NMR and ^{31}P{^{1}H} NMR spectra. In order to confirm protonation of the encapsulated guest, a number of NMR experiments were performed. In D_2O, the ^{31}P{^{1}H} NMR spectrum shows a 1:1:1 triplet with $^{1}J_{DP} = 74$ Hz. If the solvent is changed to H_2O, the ^{31}P{^{1}H} NMR spectrum shows a singlet which splits into a doublet of multiplets with $^{1}J_{HP} = 490$ Hz if the decoupler is turned off. The change in the coupling constants between H_2O and D_2O are consistent with the gyromagnetic ratios for hydrogen ($\gamma_H = 2.675 \times 10^8$ rad T^{-1} s^{-1}) and deuterium ($\gamma_D = 0.411 \times 10^8$ rad T^{-1} s^{-1}). The coupling constants are consistent with a one-bond P−H coupling, thereby confirming protonation of the encapsulated phosphine (Figure 3). In order to establish that the guests were still protonated when the pH of the solution was higher than the pK_a of the guest in water, the ^{31}P{^{1}H} NMR spectrum of DMPE (1,2-*bis*(dimethylphosphino)ethane) was monitored as a function of pD.[38] The pK_a of DMPE, which is calculated from

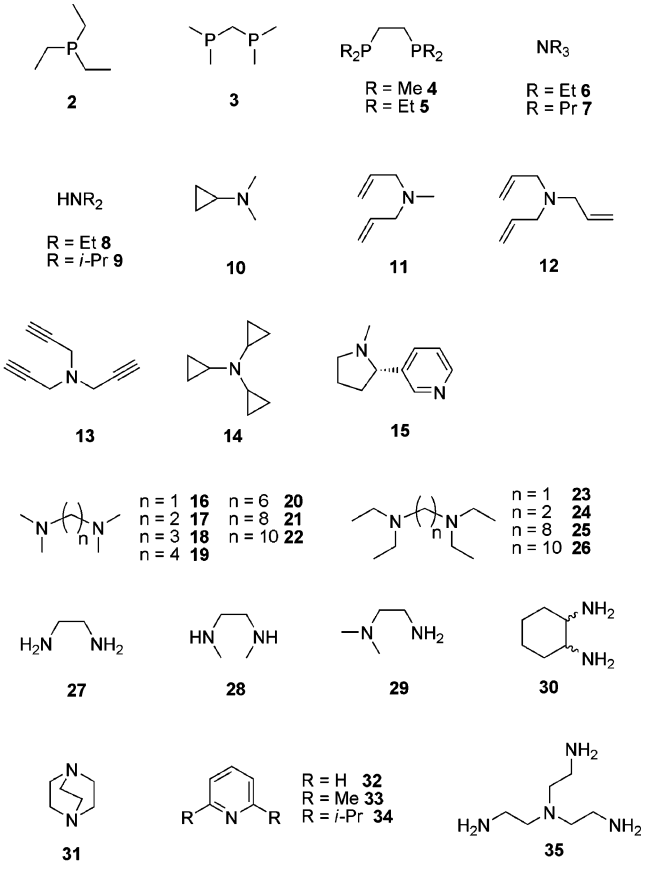

Figure 4. Scope of amines and phosphines screened as guests in **1**.

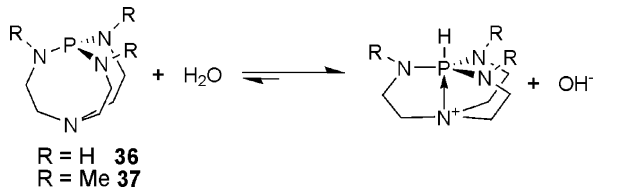

Figure 5. Schematic showing the protonation of the pro-azaphosphatranes.

the enthalpies of protonation to be about 8.5 in H_2O, is similar to that of the diamine analogue, *N*,*N*,*N*′,*N*′-tetramethylethylenediamine, which has a pK_a of 9.8.[39−42] At each pD, ranging from 7 to 13, the characteristic 1:1:1 triplet with $^{1}J_{DP} = 74$ Hz was observed, confirming deuteration and showing that the phosphine remains deuterated at pD values well above its aqueous pK_a.

Scope of Guest Encapsulation. In order to probe the scope of guests that could be encapsulated in **1** through protonation, a number of potential guests were screened with **1** (Figure 4). From the amines investigated, a number of trends are observed. Chelating tertiary amines (**16**−**20**, **23**, **24**) are cleanly encapsulated even when the chelate ring formed is relatively large. When the alkyl chain between the amines is lengthened to eight or more methylene units (**21**, **22**, **25**, **26**), encapsulation is no longer observed. Diamines unable to chelate, such as **31**, are not encapsulated. For tertiary monoamines, encapsulation is observed if the amines are sufficiently basic and maintain

(38) The phosphine DMPM was not used for these pH studies due to the acidic methylene protons on the chelate backbone.
(39) Bush, R. C.; Angelici, R. J. *Inorg. Chem.* **1988**, *27*, 681−686.
(40) Henderson, W. A.; Streuli, C. A. *J. Am. Chem. Soc.* **1960**, *82*, 5791−5794.
(41) Sowa, J. R.; Angelici, R. J. *Inorg. Chem.* **1991**, *30*, 3534−3537.
(42) Streuli, C. A. *Anal. Chem.* **1960**, *32*, 985−987.

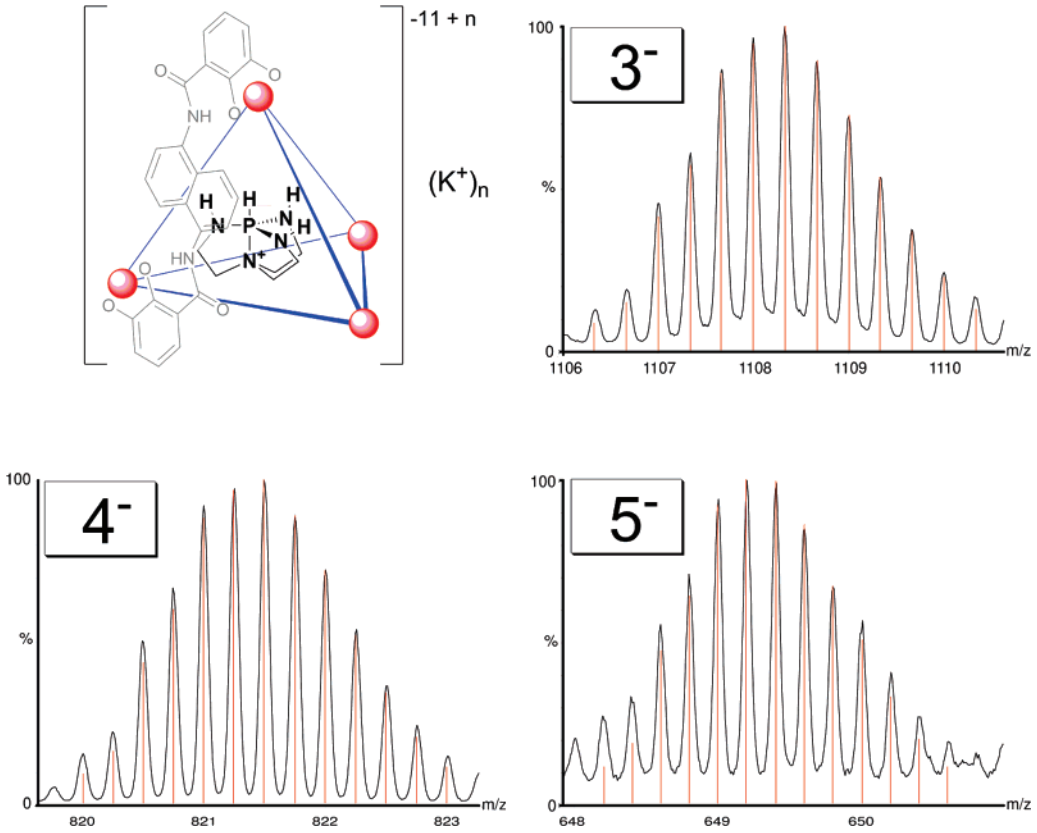

Figure 6. Representative mass spectrometry data for the host−guest complex K_8[**36**-H^+ ⊂ **1**]$^{3-}$, K_7[**36**-H^+ ⊂ **1**]$^{4-}$, and K_6[**36**-H^+ ⊂ **1**]$^{5-}$. The calculated spectra are overlaid in red.

sufficient aliphatic character. For example, triethylamine (**6**) is encapsulated, but the resonances are broad, suggesting fast guest exchange on the NMR time scale. However, a more bulky amine, tri(*n*-propyl)amine (**7**), forms a clean host−guest complex showing diastereotopic splitting of the methylene groups. Similar trends are observed for secondary amines. Diethylamine (**8**) is not encapsulated, whereas the more bulky diisopropylamine (**9**) forms a clean host−guest complex. Another observed trend is that primary amines, either monodentate or chelating (**27**−**30**, **35**), are not encapsulated. Since primary amines are more highly solvated in aqueous solution, we infer that the enthalpy loss from desolvation during encapsulation may outweigh the entropic gain of encapsulation.[43] Similarly, pyridine-based amines (**32**−**34**), ranging from pyridine to the more sterically bulky 2,6-diisopropylpyridine, are not encapsulated, presumably either because they are inherently too weakly basic or too highly solvated.

With a variety of amine and phosphine bases encapsulated in **1** we hoped to obtain further evidence for encapsulation through mass spectrometry. However, we were unable to obtain suitable mass spectrometry data for amines or phosphines encapsulated in **1** under conditions previously reported for guests in **1**.[44] In all cases, the only signals observed corresponded to empty **1**, suggesting that **1** was still intact but the guest had been ejected. Guest ejection is reversible and entropically disfavored in solution due to the solvent organization required to solvate the guest molecule. However, in the gas phase, guest ejection is entropically favorable and essentially irreversible, which may explain the difficulty in obtaining suitable data. In order to obtain mass spectrometry data of encapsulated protonated guests, more sterically bulky guests were sought to slow the rate of guest ejection. The nonanionic pro-azaphosphatranes (Figure 5) developed by Verkade and co-workers[45−48] were chosen due to their rigidity and high basicity. These "superbases" have been studied in detail and extensively characterized in the solid state and in solution. Furthermore, the pro-azaphosphatranes have been used for stoichiometric and catalytic reactions.[48−50] Upon protonation at phosphorus, donation of electron density from the axial nitrogen to the phosphorus forms the trigonal bipyramidal geometry of the azaphosphatrane with the formal cationic charge residing on the quaternized axial nitrogen. The azaphosphatranes are extremely basic, with pK_a's between 26.8 and 29.6 in DMSO,[46] and the enhanced steric bulk of these compounds should raise the barrier for guest ejection, thus enhancing the gas-phase kinetic stability of the host−guest complexes.

Two pro-azaphosphatranes **36** and **37** were encapsulated in **1** upon protonation and were confirmed to be protonated by $^{31}P\{^1H\}$ and ^{31}P NMR. Furthermore, electrospray mass spectrometry confirmed the presence of intact host−guest complexes for [**36**-H^+ ⊂ **1**]$^{11-}$ and [**37**-H^+ ⊂ **1**]$^{11-}$ in the gas phase (Figure 6). Host−guest complexes were observed in the 3^-, 4^-, and

(43) Schalley, C. A. *Mass Spectrom. Rev.* **2001**, *20*, 253−309.
(44) Andersen, U. N.; Seeber, G.; Fiedler, D.; Raymond, K. N.; Lin, D.; Harris, D. *J. Am. Soc. Mass. Spectrom.* **2006**, *17*, 292−296.
(45) Laramay, M. A. H.; Verkade, J. G. *J. Am. Chem. Soc.* **1990**, *112*, 9421−9422.
(46) Verkade, J. G. *Acc. Chem. Res.* **1993**, *26*, 483−489.
(47) Lensink, C.; Xi, S. K.; Daniels, L. M.; Verkade, J. G. *J. Am. Chem. Soc.* **1989**, *111*, 3478−3479.
(48) Kisanga, P. B.; Verkade, J. G. *Tetrahedron* **2001**, *57*, 467−475.
(49) Tang, J.-S.; Verkade, J. G. *J. Org. Chem.* **1994**, *59*, 7793−7802.
(50) Wang, Z.; Verkade, J. G. *Tetrahedron Lett.* **1988**, *39*, 9331.

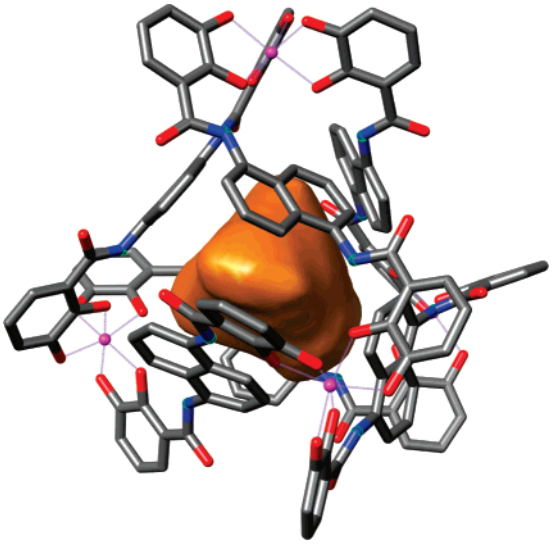

Figure 7. Representation of **1** showing the solvent-accessible surface of the cavity.

5^- charge states due to loss of K^+ in the gas phase. In all cases, the observed masses and isotope patterns match the calculated values.

Having established that protonation of the amines and phosphines allows for encapsulation, more information on the nature of the interaction of the protonated guest with **1** was sought. While the interior of **1** is predominantly defined by the hydrophobic naphthalene walls, the catecholate oxygens around each metal vertex provide a possible additional site of interaction for the guest. In order to probe the availability of the catecholate oxygens to an encapsulated guest, the shape of the interior cavity of **1** was modeled using data from the crystal structure[25] of $K_5(NEt_4)_6[NEt_4 \subset \mathbf{1}]$. Removal of the encapsulated guest from the model's interior allowed the total volume and shape of the interior cavity to be calculated using the Voidoo program.[51−53] The solvent-accessible interior cavity of **1** was mapped with a 1.4-Å diameter rolling probe, which showed that the Ga^{3+} vertices of **1** are too crowded by the ligands to be accessible by solvent (Figure 7). Examination of the solvent-accessible surface establishes that the naphthalene walls define the interior cavity. The catecholate oxygens are located in the solvent-inaccessible vertices of **1** and are predicted to be too far away from the accessible surface for interaction with a guest.

Further evidence for the lack of interaction of the guest with the catecholate oxygens was obtained from a 2D ^{1}H NOESY spectrum of encapsulated amines in **1**. Since it reflects through-space rather than through-bond interactions, the NOE experiment shows the relative proximity of the guest to different moieties of **1**. Cross-peaks in the NOESY spectrum are only seen between the encapsulated protonated guest and the naphthalene resonances of **1**; no NOEs are observed between the guest and the catechol protons (Figure 8). This confirms the results from the modeling: that the guest does not interact with the catecholate oxygens, supporting the conclusion that the hydrophobic

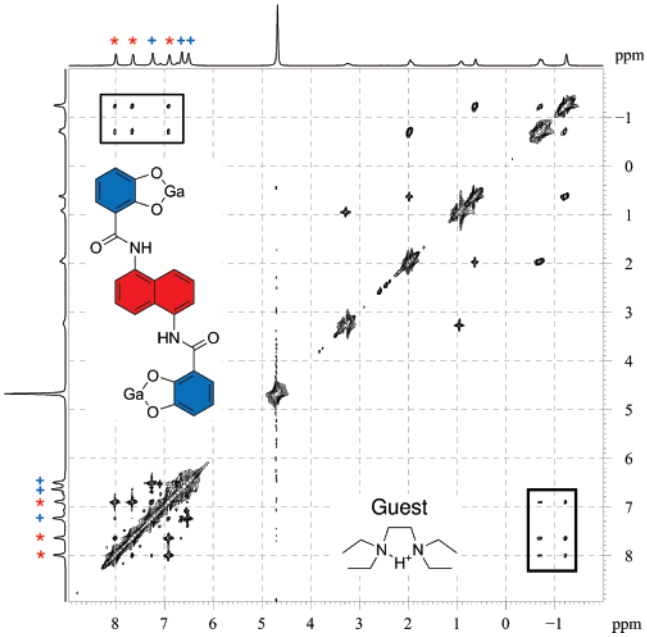

Figure 8. 2D ^{1}H NOESY of $[\mathbf{24\text{-}H}^+ \subset \mathbf{1}]^{11-}$ in D_2O with 100 ms mixing time. Cross-peaks between the host and guest are highlighted. The protons of **1** are color coded: naphthalene (red *), catecholate (blue +).

environment provided by the naphthalene rings is the predominant contributor to the interior cavity of **1**.

Guest Exchange Dynamics. In order to confirm that the amines were exchanging and that **1** was not acting as a kinetic trap for encapsulated substrates, the self-exchange rates of the protonated amine guests were determined using the selective inversion recovery (SIR) method (Figure 9).[54−56] The exchange rates were measured at 4.0 °C with 11 mM **1** and 55 mM amine at pD = 13.0 with 500 mM KCl to ensure uniform ionic strength (Table 1).

Measurement of the self-exchange rates for amines showed that the amines were exchanging quickly on the NMR time scale and that **1** is not acting as a kinetic trap. Interestingly, the exchange rate does not seem to be affected by basicity and is more greatly affected by the size of the amine. This effect is consistent with a constrictive binding mechanism for guest encapsulation in which the rate-limiting barrier for guest ejection is primarily affected by the sterics of the guest, rather than the thermodynamic binding affinity of the guest.[69] For example, **6** and **7** have essentially the same basicities, but the rates of exchange vary by two orders of magnitude. Interestingly, the exchange rate for **20** is faster than the exchange rate for smaller

(51) Kleywegt, G. J.; Jones, T. A. *Acta Crystallogr.* **1994**, *D50*, 178−185.
(52) Kleywegt, G. J.; Zou, J. Y.; Kjeldgaard, M.; Jones, T. A. In *Crystallography of Biological Macromolecules*; Rossmann, M. G., Arnold, E., Eds.; International Tables for Crystallography, Vol. F.; Kluwer: Dordrecht, London, 2001; Chapter 17.1, pp 353−356 and 366−367.
(53) Molecular graphics images were produced using the UCSF Chimera package from the Resource for Biocomputing, V. and Informatics at the University of California, San Francisco (supported by NIH P41 RR-01081).
(54) Bain, A.; Cramer, J. A. *J. Magn. Reson., Ser. A* **1993**, *103*, 217−222.
(55) Bain, A. D.; Cramer, J. A. *J. Magn. Reson., Ser. A* **1996**, *118*, 21−27.
(56) Perrin, C. L.; Dwyer, T. J. *Chem. Rev.* **1990**, *90*, 935−967.
(57) Chawla, B.; Mehta, S. K. *J. Phys. Chem. B* **1984**, *88*, 2650−2655.
(58) Fowler, R. T. *J. Appl. Chem.* **1954**, *4*, 449−452.
(59) Hall, N. F.; Sprinkle, M. R. *J. Am. Chem. Soc.* **1932**, *54*, 3469−3485.
(60) Gustafson, R. L.; Martell, A. E. *J. Am. Chem. Soc.* **1959**, *81*, 525−529.
(61) Monjoint, P.; Ruasse, M.-F. *Tetrahedron Lett.* **1984**, *25*, 3183−3186.
(62) Lewin, A. H.; Sun, G.; Fudala, L.; Navarro, H.; Zhou, L.-M.; Popik, P.; Faynsteyn, A.; Skolnick, P. *Med. Chem.* **1998**, *41*, 988−995.
(63) Titrated in this work.
(64) Leyden, M., Jr. *J. Phys. Chem. B* **1971**, *75*, 2400.
(65) Vexlearschi, G. *Bull. Soc. Chim. Fr.* **1956**, 589−596.
(66) Vexlearschi, G.; Rumpf, P. *Compte Rendus* **1953**, *236*, 939−942.
(67) Gero, A. *J. Am. Chem. Soc.* **1954**, *76*, 5158−5159.
(68) Gillaspy, M.; Lefker, B. A.; Hada, W. A.; Hoover, D. J. *Tetrahedron Lett.* **1995**, *36*, 7399−7402.
(69) Pluth, M. D.; Raymond, K. N. *Chem. Soc. Rev.* **2007**, *36*, 161−171.

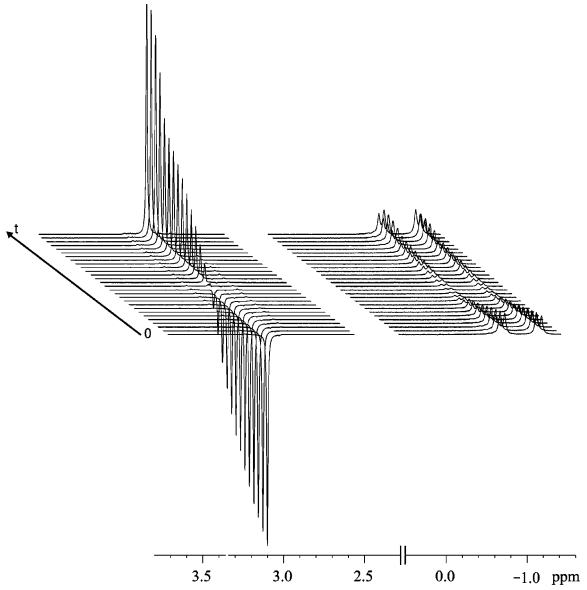

Figure 9. Selective inversion recovery experiment for **13**. The delay time between the selective inversion centered at the exterior guest (3 ppm) and the acquisition spectrum increases from bottom to top. The spin saturation is transferred to the encapsulated guest through chemical exchange, resulting in a decreased intensity in the guest signals (at −1 ppm).

Table 1. Self-Exchange Rates and pK_a's for Selected Encapsulated Amines

amine[a]	pK_a	k_{277} (s^{-1})	amine[a]	pK_a	k_{277} (s^{-1})[d]
6[57]	10.7	46(9)	**15**[58]	10.6	1.0(5)
7[59]	10.7	0.31(4)	**17**[60]	9.1	47(9)
9[61]	10.8	17(3)[b]	**18**[62]	9.8	1.1(2)
10[63]	8.5	5.3(3)	**19**[64]	9.8	0.24(3)[c]
12[65]	8.3	5.4(6)	**20**[64]	9.8	1.9(3)
13[66]	8.1	4.4(6)	**24**[67]	10.8	0.13(2)[c]
14[68]	6.4	1.1(1)			

[a] The pK_a references are denoted with superscripts. [b] Measured at 1.1 mM **1** and 5.5 mM **9** due to low solubility. [c] Exchange rate too slow to measure at 277 K; reported values were measured at 320 K. [d] The exchange rates for substrates **11** and **23** were too fast to measure using the SIR method at 277 K.

analogues such as **18** or **19**. The larger alkyl backbone of **20** may disfavor chelation inside of **1** and allow for more facile exchange. For amines **19** and **24**, the slow rates of self-exchange allowed the activation parameters of the self-exchange process to be determined. The activation parameters for guest exchange of **19** were $\Delta G^{\ddagger}_{298} = 19(2)$ kcal/mol, $\Delta H^{\ddagger} = 10.8(9)$ kcal/mol, $\Delta S^{\ddagger} = -28(4)$ eu and for **24** were $\Delta G^{\ddagger}_{298} = 19.9(8)$ kcal/mol, $\Delta H^{\ddagger} = 16.7(6)$ kcal/mol, $\Delta S^{\ddagger} = -10.9(6)$ eu. These values are similar to those determined for the self-exchange activation parameters for tetraalkylammonium cations, suggesting that the same exchange pathway is operating.[27]

Thermodynamic Effects on the Basicity of Amines. All of the amines and phosphines encapsulated in Figure 4 were investigated at pH values above the pK_a of the putative guest. Of the amines encapsulated in **1**, the magnitude of the effective shift in basicity was investigated by monitoring 1:1 host−guest complexes as a function of pH.[70] Heating the host−guest complex perturbed the ratio of interior to exterior guest showing that the system was operating under fast exchange. The ratio of interior to exterior guest did not change after heating a host−guest complex to 75 °C for 24 h and returning the sample to room temperature, suggesting that the thermodynamic equilibrium ratio was already present. At pH 8, (which is the approximate pH of a 10 mM solution of **1** in unbuffered H_2O), basic amines with pK_a values over 8 are mainly protonated in solution, explaining the encapsulation of the protonated form of the amines. However, less basic amines such as **10**−**14**, which are protonated to a lesser extent at pH 8, are also cleanly encapsulated, thereby suggesting a strong cavity stabilization of the protonated form of the amines. Formally, this stabilization is a shift in the pK_a of the amine, but as we are unable to observe neutral guests inside of the assembly, it is more accurately referred to as a shift in effective basicity. The thermodynamic cycle for the encapsulation of protonated substrates is shown in Figure 10. The acid−base equilibrium of the substrate in free solution is defined by K_1, with K_2 being the binding constant of the protonated form of the substrate. From previous work, it is known that neutral substrates can enter **1**; however, the extent of the binding affinity of neutral substrates encapsulated in **1** (K_4) has remained unexplored. Although we are unable to detect the neutral substrates encapsulated in **1**, the thermodynamic cycle can be completed by including K_3, which is essentially the acid−base equilibrium for the substrate encapsulated in **1**.

(70) Phosphines were not investigated due to their low water solubility.

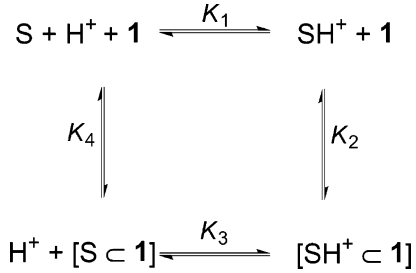

Figure 10. Schematic of the acid−base equilibrium (K_1) and the greatly favored substrate−host equilibrium (K_2).

Table 2. Binding Constants,[a] Energies, and Shifts in the Effective Basicity for Encapsulated Amines

amine	pK_a	$K_{eff(298)}$ (M^{-1})[b]	log(K_{eff})	$-\Delta G^{\circ}$ (kcal/mol)	effective basicity (pK_{eff})
6	10.7	130	2.1	2.9	12.8
7	10.7	500	2.7	3.7	13.4
9	10.8	2510	3.4	4.6	14.2
10	8.5	2080	3.3	4.5	11.8
12	8.3	25100	4.4	6.0	12.7
13	8.1	31600	4.5	6.1	12.6
14	6.4	1590	3.2	4.4	9.6
15	10.6	650	2.8	3.8	13.4
17	9.1	1260	3.1	4.2	12.2
18	9.8	6310	3.8	5.2	13.6
19	9.8	6450	3.8	5.2	13.6
20	9.8	12600	4.1	5.6	13.9
24	10.8	3160	3.5	4.8	14.3

[a] Binding constants have an estimated uncertainty of 10%. [b] Binding constants for substrates **11** and **23** were not determined due to deprotonation of the methylene hydrogens and substrate decomposition at high pH.

Like the hydrophobic effect, the guest encapsulation process is largely entropically driven due to the release of the solvent molecules upon encapsulation of the protonated guests. In solution, the cationic protonated base is more highly solvated than the neutral base, suggesting that the entropic gain due to desolvation is greater for the cationic. Furthermore, encapsulation of a cationic guest lowers the charge of **1** from −12 to

−11 which also is entropically favored due to the decreased solvation of **1**. The idea of entropically driven guest encapsulation also explains why primary amines are not encapsulated in **1**. While primary amines are highly solvated in solution, the ability of these amines to hydrogen bond with solvating water molecules increases the enthalpic contributions to solvation. In order for desolvation to occur, an enthalpic penalty must be paid in order to break the hydrogen bonds with surrounding solvent which, in the case of primary amines, outweighs the entropic forces, thereby prohibiting guest encapsulation.

The effective basicity of the encapsulated substrate (pK_{eff}) can be calculated from the product of the pK_a of the protonated amine and the binding constant (K_{eff}) of the protonated amine in **1** (Table 2). By monitoring the interior and exterior guest integrations of equimolar solutions of **1** and the amine, the binding constants of the amines were calculated using eq 1. These measurements were repeated at pH 10.5, 11.0, and 11.5 at 25.0 °C. Varying the pH affected the ratios of encapsulated to free guest, again supporting our conclusion that the substrates are protonated inside **1**.

$$K_{eff} = \frac{[SH^+ \subset \mathbf{1}]10^{-pK_a}}{[S][\mathbf{1}]10^{-pH}} \quad (1)$$

Conclusion

In summary, a variety of protonated amines and phosphines have been encapsulated in the interior of a metal−ligand assembly. We have demonstrated that the driving forces for guest encapsulation dramatically alter the effective basicities of encapsulated amines by over 4 pK_a units for a wide variety of amines. Furthermore, we have shown that the amines are freely exchanging to the exterior of the assembly, eliminating the possibility of encapsulation acting as a kinetic trap. The hydrophobic effect, specifically the entropic gain upon desolvation of the protonated bases, likely drives encapsulation. Host-mediated shifts in the effective basicities of guest molecules can potentially be exploited for a number of sensing applications where the difference in guest pK_a's can influence the relative binding affinities. Similarly, reactions involving high-energy protonated species, such as those found in many hydrolysis reactions, could potentially be greatly accelerated by transition-state stabilization upon encapsulation in suitable molecular hosts. As synthetic chemists have often mimicked enzymes and other biological systems in the formation of supramolecular architectures, these supramolecular architectures clearly can provide valuable information about the forces active inside of Nature's remarkably complex and efficient systems. Much as Nature uses changes in basicities to influence catalytic activity in enzymes, current work is underway to further exploit these shifts in basicity to facilitate catalytic reactions.

Experimental Section

General Procedures. All NMR spectra were obtained using Bruker DRX-500 or AV-500 MHz spectrometers at the indicated frequencies. Chemical shifts are reported as parts per million (δ) and referenced to residual protic solvent peaks. Proton-decoupled $^{13}C\{^1H\}$ chemical shifts were recorded at 125 MHz and referenced to an external standard of TMS. Suitable $^{13}C\{^1H\}$ spectra for the host−guest complexes could not be obtained after 8000 scans with a pre-scan delay of 2 s, and all $^{13}C\{^1H\}$ spectra were recorded using a 2D DEPT-HSQC experiment. $^{31}P\{^1H\}$ and ^{31}P NMR spectra were recorded at 202 MHz and were referenced to trimethyl phosphate (1.67 ppm). The following abbreviations are used in describing NMR couplings: (s) singlet, (d) doublet, (t) triplet, (q) quartet, (b) broad, (m) multiplet. The temperature of all variable-temperature NMR experiments was calibrated with methanol or ethylene glycol standards. The binding constants for each amine were measured in H_2O using the Watergate solvent suppression sequence at 25 °C at three different pH's (10.5, 11.0, 11.5). Selective inversion recovery (SIR) experiments were performed at constant temperature using a 10 s delay time between experiments. Data points for each SIR experiment were measured from 0.0005 s to 18 s in 42 increments. In all cases, the efficiency of the inversion pulse was greater than 70%. The raw data were fit using CIFIT, and all uncertainties in rate constants were reported as 3× the uncertainty generated by CIFIT. The protonation constant of *N*,*N*-dimethylcyclopropylamine was determined using experimental conditions and equipment previously described,[71] and the data were fit using Hyperquad.[72]

Materials. All reagents were obtained from commercial suppliers and used without purification unless otherwise noted. *N*,*N*,*N*′,*N*′-Tetramethyl-1,8-diaminooctane, *N*,*N*,*N*′,*N*′-tetramethyl-1,10-diaminodecane, and *N*,*N*,*N*′,*N*′-tetraethyl-1,10-diaminodecane were prepared from the corresponding dibromides and the necessary secondary amine following literature procedures.[73] *N*,*N*-Dimethyl cyclopropylamine[74] and tricyclopropylamine[68] were prepared as described in the literature, isolated as the HCl salt, and recrystallized from CH_2Cl_2/pentane. 2,5,8,9-Tetraaza-1-phosphabicyclo[3.3.3]undecane hydrochloride was prepared from tris(2-aminoethyl)amine and bis(diisopropylamino)chlorophosphine instead of bis(dimethyl)chlorophosphine in a procedure analogous to the procedure described in the literature.[46] The host assembly $K_{12}[Ga_4L_6]$ was prepared as described in the literature and precipitated with either acetone or ether.[22]

General Procedure for Amine/Phosphine Encapsulation. In an N_2 glovebox, 15 mg of $K_{12}[Ga_4L_6]$ was added to an NMR tube at which point 0.5 mL of D_2O was added. The amine (1.5−2 equiv) was added by syringe, and the NMR tube was shaken for 30 s. For phosphines, $K_{12}[Ga_4L_6]$ precipitated with Et_2O was used to avoid formation of cationic phosphine/acetone adducts.

General Procedure for Selective Inversion Recovery Experiments. In an N_2 glovebox, 15 mg of $K_{12}[Ga_4L_6]$ was added to an NMR tube at which point 0.5 mL of 500 mM KCl in D_2O adjusted to pH 13.0 was added. The amine (5.0 equiv) was added by syringe, and the NMR tube was shaken for 30 s.

$[PEt_3\text{-}H^+ \subset Ga_4L_6]^{11-}$ ($[2\text{-}H^+ \subset 1]^{11-}$): ^1H NMR (500 MHz, D_2O): δ 7.91 (d, J = 8.0 Hz, 12H, *aryl*), 7.64 (d, J = 8.0 Hz, 12H, *aryl*), 7.22 (d, J = 8.0 Hz, 12H, *aryl*), 6.93 (t, J = 7.4 Hz, 12H, *aryl*), 6.32 (d, J = 7.6 Hz, 12H, *aryl*), 6.55 (t, J = 7.4 Hz, 12H, *aryl*). Guest: −1.31 (m, 6H, CH_2), −1.79 (m, 12H, CH_3). $^{31}P\{^1H\}$ (D_2O, 202 MHz): δ 49.6 (t, $^1J_{PD}$ = 73 Hz,). $^{31}P\{^1H\}$ (202 MHz, H_2O): δ 50.1 (s). ^{31}P (202 MHz, H_2O): δ 50.1 (d, $^1J_{PH}$ = 486 Hz).

[Bis(dimethylphosphino)methane-$H^+ \subset Ga_4L_6]^{11-}$ ($[3\text{-}H^+ \subset 1]^{11-}$): ^1H NMR (500 MHz, D_2O): δ 7.96 (bs, 12H, *aryl*), 7.86 (bs, 12H, *aryl*), 7.25 (bd, 12H, *aryl*), 7.02 (bd, 12H, *aryl*), 6.84 (bs, 12H, *aryl*), 6.59 (bs, 12H, *aryl*). Guest: −0.89 (dd, $^2J_{PH}$ = 31.5 Hz, $^3J_{HH}$ = 15.0 Hz, 2H, CH_2), −1.62 (d, $^2J_{PH}$ = 31.5 Hz, 12H). $^{31}P\{^1H\}$ (D_2O, 202 MHz): δ 32.1 (t, $^1J_{PD}$ = 74.9 Hz,). ^{31}P (202 MHz, D_2O): δ 32.1 (tm, $^1J_{PD}$ = 74.8 Hz, $^2J_{PH}$ = 14.2 Hz). $^{31}P\{^1H\}$ (202 MHz, H_2O): δ 34.0 (s). ^{31}P (202 MHz, H_2O): δ 34.0 (dm, $^1J_{PH}$ = 489 Hz, $^2J_{PH}$ = 14.4 Hz).

[Bis(dimethylphosphino)ethane-$H^+ \subset Ga_4L_6]^{11-}$ ($[4\text{-}H^+ \subset 1]^{11-}$): ^1H NMR (500 MHz, D_2O): δ 8.01 (d, J = 7.5 Hz, 12H, *aryl*), 7.75 (d, J = 8.5 Hz, 12H, *aryl*), 7.28 (d, J = 8.0 Hz, 12H, *aryl*), 7.04 (t, J = 8.0 Hz, 12H, *aryl*), 6.74 (d, J = 7.0 Hz, 12H, *aryl*), 6.58 (t, J = 8.0 Hz, 12H, *aryl*). Guest: −0.63 (s, 6H, P−CH_3), −0.83 (s, 6H, P−CH_3),

(71) Johnson, A. R.; O'Sullivan, B.; Raymond, K. N. *Inorg. Chem.* **2000**, *39*, 2652−2660.
(72) Gans, P.; Sabatini, A.; Vacca, A. *Talanta* **1996**, *43*, 1739−1752.
(73) Souirti, S.; Baboulene, M. *Can. J. Chem.* **2001**, *79*, 1153−1158.
(74) Chaplinski, V.; de Meijere, A. *Angew. Chem., Int. Ed.* **1996**, *35*, 413−414.

−1.17 (bs, 2H, CH_2), −1.39 (bs, 2H, CH_2), −1.64 (s, 3H, P−CH_3), −1.76 (s, 3H, P−CH_3). $^{31}P\{^1H\}$ (202 MHz, H_2O): δ −3.8 (d, J = 33 Hz). ^{31}P (202 MHz, H_2O): δ 14.2 (dm, J = 487 Hz). ^{31}P (202 MHz, D_2O): δ −3.8 (td, J = 74 Hz, 33 Hz).

[Bis(diethylphosphino)ethane-H$^+$ ⊂ Ga$_4$L$_6$]$^{11-}$ ([5-H$^+$ ⊂ 1]$^{11-}$): ^1H NMR (500 MHz, D_2O): δ 8.09 (d, J = 7.5 Hz, 12H, *aryl*), 7.72 (d, J = 9.0 Hz, 12H, *aryl*), 7.18 (d, J = 8.0 Hz, 12H, *aryl*), 7.00 (t, J = 7.5 Hz, 12H, *aryl*), 6.84 (d, J = 7.0 Hz, 12H, *aryl*), 6.61 (t, J = 8.0 Hz, 12H, *aryl*). Guest: −0.29 (m, J = 9.0 Hz, 6H, CH_3), −0.78 (m, J = 9.0 Hz, 6H, CH_3), −0.88 (m, J = 8.0 Hz, 8H, CH_2), −1.40 to −1.85 (bm, 4H, CH_2). $^{31}P\{^1H\}$ (202 MHz, D_2O): δ 14.2 (td, $^1J_{PD}$ = ∼80 Hz) $^{31}P\{^1H\}$ (202 MHz, H_2O): δ 14.2 (d, J = 38 Hz). ^{31}P (202 MHz, H_2O): δ 14.2 (dm, J = 488 Hz).

[NEt$_3$-H$^+$ ⊂ Ga$_4$L$_6$]$^{11-}$ ([6-H$^+$ ⊂ 1]$^{11-}$): ^1H NMR (500 MHz, D_2O): δ 8.97 (bs, 12H, *aryl*), 7.77 (d, J = 7.6 Hz, 12H, *aryl*), 7.28 (d, J = 7.4 Hz, 12H, *aryl*), 7.04 (bs, 12H, *aryl*), 6.72 (d, J = 7.0 Hz, 12H, *aryl*), 6.57 (t, J = 7.5 Hz, 12H, *aryl*). Guest: −0.76 (bs, 6H, CH_2), −1.81 (bs, 9H, CH_3). $^{13}C\{^1H\}$ NMR (125 MHz, D_2O): δ 43.3 (CH_2), 8.1 (CH_3).

[N(*n*-Pr)$_3$-H$^+$ ⊂ Ga$_4$L$_6$]$^{11-}$ ([7-H$^+$ ⊂ 1]$^{11-}$): ^1H NMR (500 MHz, D_2O): δ 8.05 (bs, 12H, *aryl*), 7.65 (d, J = 7.5 Hz, 12H, *aryl*), 7.31 (d, J = 8.5 Hz, 12H, *aryl*), 7.15 (bs, 12H, *aryl*), 6.86 (d, J = 7.5 Hz, 12H, *aryl*), 6.57 (t, J = 7.5 Hz, 12H, *aryl*). Guest: −0.57 (d, J = 117 Hz, 6H, N−CH_2), −1.38 (t, J = 6.5 Hz, CH_3), −1.61 (d, J = 117 Hz, NCH_2CH_2). $^{13}C\{^1H\}$ NMR (125 MHz, D_2O): δ 51.9 (CH_2), 16.9 (CH_2), 7.8 (CH_3).

[HN(*i*-Pr)$_2$-H$^+$ ⊂ Ga$_4$L$_6$]$^{11-}$ ([8-H$^+$ ⊂ 1]$^{11-}$): ^1H NMR (500 MHz, D_2O): δ 8.00 (d, J = 8.0 Hz, 12H, *aryl*), 7.91 (d, J = 8.0 Hz, 12H, *aryl*), 7.31 (d, J = 8.0 Hz, 12H, *aryl*), 7.04 (t, J= 7.5 Hz, 12H, *aryl*), 6.73 (d, J = 8.0 Hz, 12H, *aryl*), 6.58 (d, J = 7.5 Hz, 12H, *aryl*). Guest: −0.79 (s, 1H, N−C*H*Me$_2$), −1.68 (bs, 6H, NCH(CH_3)$_2$). $^{13}C\{^1H\}$ NMR (125 MHz, D_2O): δ 44.2 (CH), 17.4 (CH_3).

[*N*,*N*-Dimethyl cyclopropylamine-H$^+$ ⊂ Ga$_4$L$_6$]$^{11-}$ ([10-H$^+$ ⊂ 1]$^{11-}$): ^1H NMR (500 MHz, D_2O): δ 7.81 (d, J = 7.5 Hz, 12H, *aryl*), 7.70 (d, J = 9.0 Hz, 12H, *aryl*), 7.12 (d, J = 8.0 Hz, 12H, *aryl*), 6.90 (t, J = 7.5 Hz, 12H, *aryl*), 6.63 (d, J = 7.0 Hz, 12H, *aryl*), 6.46 (t, J = 8.0 Hz, 12H, *aryl*). Guest: −0.78 (s, 6H, CH_3), −1.71 (bm, 3H, CH_2 and CH), −2.67 (bm, 2H, CH_2). $^{13}C\{^1H\}$ NMR (125 MHz, D_2O): δ 41.8 (CH), 37.6 (CH_3), −1.2 (CH_2).

[*N*,*N*-Diallyl methylamine-H$^+$ ⊂ Ga$_4$L$_6$]$^{11-}$ ([11-H$^+$ ⊂ 1]$^{11-}$): ^1H NMR (500 MHz, D_2O): δ 7.87 (bs, 12H, *aryl*), 7.68 (d, J = 8.5 Hz, 12H, *aryl*), 7.18 (bs, 12H, *aryl*), 6.91 (t, J = 8.0 Hz, 12H, *aryl*), 6.64 (d, J = 8.0 Hz, 12H, *aryl*), 6.48 (bs, 12H, *aryl*). Guest: 3.7 (bm, 3H, C*H*═CH_2), 2.7 (bm, 6H, CH═CH_2), −0.36 to −0.91 (bd, J = 274 Hz, 6H, CH_2), −1.73 (s, 3H, CH_3) $^{13}C\{^1H\}$ NMR (125 MHz, D_2O): δ 131.3 (*C*H═CH_2), 114.1 (═CH_2), 55.6 (CH_2), 35.6 (CH_3).

[Triallylamine-H$^+$ ⊂ Ga$_4$L$_6$]$^{11-}$ ([12-H$^+$ ⊂ 1]$^{11-}$): ^1H NMR (500 MHz, D_2O): δ 8.04 (bs, 12H, *aryl*), 7.81 (d, J = 7.5 Hz, 12H, *aryl*), 7.25 (m, 12H, *aryl*), 7.00 (bs, 12H, *aryl*), 6.75 (d, J = 7.5 Hz, 12H, *aryl*), 6.58 (t, J = 7.0 Hz, 12H, *aryl*). Guest: 3.81 (d, J = 10 Hz, 3H, CH), 2.65 (d, J = 16.5 Hz, 3H, CH), 2.31 (bm, 3H, CH), −0.15 (bs, 6H, CH_2). $^{13}C\{^1H\}$ NMR (125 MHz, D_2O): δ 125.9 (═CH), 113.1 (═CH_2), 52.4 (CH_2).

[Tripropargylamine-H$^+$ ⊂ Ga$_4$L$_6$]$^{11-}$ ([13-H$^+$ ⊂ 1]$^{11-}$): ^1H NMR (500 MHz, D_2O): δ 7.67 (d, J = 8.0 Hz, 12H, *aryl*), 7.61 (d, J = 7.5 Hz, 12H, *aryl*), 7.12 (d, J = 7.8 Hz, 12H, *aryl*), 6.88 (t, J = 7.7 Hz, 12H, *aryl*), 6.61 (d, J = 8.0 Hz, 12H, *aryl*), 6.45 (t, J = 7.8 Hz, 12H, *aryl*). Guest: −0.45 (dd, J = 97 Hz, J = 14 Hz, 6H, CH_2), −0.82 (bs, 3H, CH).

[Tricyclopropylamine-H$^+$ ⊂ Ga$_4$L$_6$]$^{11-}$ ([14-H$^+$ ⊂ 1]$^{11-}$): ^1H NMR (500 MHz, D_2O): δ 7.65 (d, J = 7.5 Hz, 12H, *aryl*), 7.58 (d, J = 7.5 Hz, 12H, *aryl*), 7.01 (d, J = 7.4 Hz, 12H, *aryl*), 6.81 (t, J = 7.6 Hz, 12H, *aryl*), 6.51 (d, J = 8.0 Hz, 12H, *aryl*), 6.35 (t, J = 7.6 Hz, 12H, *aryl*). Guest: −0.82 to −0.98 (bm, 6H, CH_2), −1.7 to −2.3 (bm, 6H, CH_2), −2.72 (bs, 3H, CH).

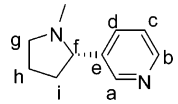

[(−)-Nicotine-H$^+$ ⊂ Ga$_4$L$_6$]$^{11-}$ ([15-H$^+$ ⊂ 1]$^{11-}$): ^1H NMR (500 MHz, D_2O): δ 7.97 (bs, 12H, *aryl*), 7.71 (bs, 12H, *aryl*), 7.17 (bs, 12H, *aryl*), 6.91 (bs, 12H, *aryl*), 6.78 (bs, 12H, *aryl*), 6.50 (bs, 12H, *aryl*). Guest: 5.59 (m, 1H, H_b), 5.52 (m, 1H, H_c), 4.87 (s, 1H, H_a), 3.58 (m, 1H, H_d), 0.00 (m, 4H, CH_3 and H_f), −0.26 (bm, 1H, H_g(A)), −0.49 (m, 1H, H_i(A)), −0.71 (m, 1H, H_i(B)), −0.76 (m, 1H, H_g(B)), −1.05 (m, 1H, H_h(A)), −1.42 (m, 1H, H_h(B)). $^{13}C\{^1H\}$ NMR (125 MHz, D_2O): δ 145.8 (C_a, C_b), 134.0 (C_d), 119.4 (C_c), 64.8 (C_f), 54.7 (C_g), 37.1 (CH_3), 31.2 (C_i), 16.0 (C_h).

[*N*,*N*,*N*′,*N*′-Tetramethyldiaminomethane-H$^+$ ⊂ Ga$_4$L$_6$]$^{11-}$ ([16-H$^+$ ⊂ 1]$^{11-}$): ^1H NMR (500 MHz, D_2O): δ 7.81 (d, J = 7.6 Hz, 12H, *aryl*), 7.67 (d, J = 8.2 Hz, 12H, *aryl*), 7.16 (d, J = 7.0 Hz, 12H, *aryl*), 6.89 (t, J = 8.1 Hz, 12H, *aryl*), 6.60 (d, J = 7.0 Hz, 12H, *aryl*), 6.46 (t, J = 7.4 Hz, 12H, *aryl*). Guest: −0.52 (bs, 14H, N−CH_3 and N−CH_2). $^{13}C\{^1H\}$ NMR (125 MHz, D_2O): δ 89.6 (CH_2), 38.3 (CH_3).

[*N*,*N*,*N*′,*N*′-Tetramethylethylenediamine-H$^+$ ⊂ Ga$_4$L$_6$]$^{11-}$ ([17-H$^+$ ⊂ 1]$^{11-}$): ^1H NMR (500 MHz, D_2O): δ 7.98 (d, J = 7.6 Hz, 12H, *aryl*), 7.77 (d, J = 9.5 Hz, 12H, *aryl*), 7.30 (dd, J = 7.0 Hz, 1.0 Hz, 12H, *aryl*), 7.04 (t, J = 8.1 Hz, 12H, *aryl*), 6.74 (d, J = 7.0 Hz, 12H, *aryl*), 6.57 (t, J = 7.7 Hz, 12H, *aryl*). Guest: −0.52 (bs, 12H, N−CH_3), −0.83 (bm, 4H, CH_2). $^{13}C\{^1H\}$ NMR (125 MHz, D_2O): δ 49.9 (CH_2), 39.7 (CH_3).

[*N*,*N*,*N*′,*N*′-Tetramethyl-1,3-propanediamine-H$^+$ ⊂ Ga$_4$L$_6$]$^{11-}$ ([18-H$^+$ ⊂ 1]$^{11-}$): ^1H NMR (500 MHz, D_2O): δ 7.98 (bs, 12H, *aryl*), 7.84 (d, J = 7.5 Hz, 12H, *aryl*), 7.33 (d, J = 8.5 Hz, 12H, *aryl*), 7.06 (bs, 12H, *aryl*), 6.80 (d, J = 7.5 Hz, 12H, *aryl*), 6.64 (bs, 12H, *aryl*). Guest: −0.46 (s, 12H, N−CH_3), −0.65 (dm, J = 17.2 Hz, 7.0 Hz, 4H, N−CH_2), −1.39 (quintet, J = 6.0 Hz, 2H, $NCH_2CH_2CH_2N$). $^{13}C\{^1H\}$ NMR (125 MHz, D_2O): δ 39.5 (CH_3), 15.2 (CH_2).

[*N*,*N*,*N*′,*N*′-Tetramethyl-1,4-butanediamine-H$^+$ ⊂ Ga$_4$L$_6$]$^{11-}$ ([19-H$^+$ ⊂ 1]$^{11-}$): ^1H NMR (500 MHz, D_2O): δ 7.93 (d, J = 8.0 Hz, 12H, *aryl*), 7.86 (d, J = 8.5 Hz, 12H, *aryl*), 7.34 (d, J = 7.5 Hz, 12H, *aryl*), 7.06 (t, J = 8.5 Hz, 12H, *aryl*), 6.80 (d, J = 7.5 Hz, 12H, *aryl*), 6.64 (bs, 12H, *aryl*). Guest: −0.42 (s, 6H, $N(CH_3)_2$), −0.86 (s, 6H, $N(CH_3)_2$), −1.18 (s, 4H, CH_2), −1.44 (bd, J = 20 Hz, 4H, CH_2). $^{13}C\{^1H\}$ NMR (125 MHz, D_2O): δ 54.2 (CH_2), 39.8 (CH_3), 22.2 (CH_2).

[*N*,*N*,*N*′,*N*′-Tetramethyl-1,6-hexanediamine-H$^+$ ⊂ Ga$_4$L$_6$]$^{11-}$ ([20-H$^+$ ⊂ 1]$^{11-}$): ^1H NMR (500 MHz, D_2O): δ 7.90 (d, J = 8.5 Hz, 12H, *aryl*), 7.65 (d, J = 8.5 Hz, 12H, *aryl*), 7.35 (d, J = 8.5 Hz, 12H, *aryl*), 7.02 (t, J = 8.0 Hz, 12H, *aryl*), 6.84 (d, J = 7.5 Hz, 12H, *aryl*), 6.61 (t, J = 7.5 Hz, 12H, *aryl*). Guest: −0.53 (s, 12H, N−Me), −0.93 to −1.03 (bm, 8H, CH_2), −2.14 (s, 4H, CH_2). $^{13}C\{^1H\}$ NMR (125 MHz, D_2O): δ 52.0 (N−CH_2), 40.0 (N−CH_3), 19.8 (CH_2), 19.6 (CH_2), 15.6 (CH_2).

[*N*,*N*,*N*′,*N*′-Tetraethyldiaminomethane-H$^+$ ⊂ Ga$_4$L$_6$]$^{11-}$ ([23-H$^+$ ⊂ 1]$^{11-}$): ^1H NMR (500 MHz, D_2O): δ 7.92 (d, J = 7.2 Hz, 12H, *aryl*), 7.63 (d, J = 8.0 Hz, 12H, *aryl*), 7.18 (d, J = 7.9 Hz, 12H, *aryl*), 6.88 (t, J = 8.0 Hz, 12H, *aryl*), 6.63 (d, J = 6.8 Hz, 12H, *aryl*), 6.46 (t, J = 7.6 Hz, 12H, *aryl*). Guest: −0.65 to −0.83 (bm, 8H, N−CH_2), −1.31 to −1.54 (bm, 12H, CH_3). $^{13}C\{^1H\}$ NMR (125 MHz, D_2O): δ 80.6 (CH_2), 41.5 (CH_2), 8.7 (CH_3).

[*N*,*N*,*N*′,*N*′-Tetraethylethylenediamine-H$^+$ ⊂ Ga$_4$L$_6$]$^{11-}$ ([24-H$^+$ ⊂ 1]$^{11-}$): ^1H NMR (500 MHz, D_2O): δ 8.01 (bs, 12H, *aryl*), 7.74 (bs, 12H, *aryl*), 7.34 (bs, 12H, *aryl*), 7.00 (bs, 12H, *aryl*), 6.75 (d, J = 7.5 Hz, 12H, *aryl*), 6.61 (bs, 12H, *aryl*). Guest: −0.57 to −0.64 (bm, 12H, N−CH_2), −1.12 (s, 12H, CH_3). $^{13}C\{^1H\}$ NMR (125 MHz, D_2O): δ 44.8 (CH_2), 9.3 (CH_3).

[2,5,8,9-Tetraaza-1-phosphabicyclo[3.3.3]undecane-H$^+$ ⊂ Ga$_4$L$_6$]$^{11-}$ ([36-H$^+$ ⊂ 1]$^{11-}$): ^1H NMR (500 MHz, D_2O): δ 7.87 (d, J = 7.5 Hz, 12H, *aryl*), 7.76 (d, J = 8.0 Hz, 12H, *aryl*), 7.19 (d, J = 8.0 Hz, 12H, *aryl*), 7.03 (t, J = 7.5 Hz, 12H, *aryl*), 6.40 (d, J = 7.5 Hz, 12H, *aryl*),

6.49 (t, $J = 7.5$ Hz, 12H, *aryl*). Guest: 0.79 (s, 6H, CH_2), −1.00 (s, 6H, CH_2). $^{31}P\{^1H\}$ (202 MHz, H_2O): δ −48.6 (s). ^{31}P (202 MHz, H_2O): δ −48.6 (d, $J = 487$ Hz). TOF MS ES(−) (MeOH), ◆ = $[Ga_4L_6]^{12-}$, calcd (found), *m*/*z*: 1108.348 (1108.334) [◆ + **36**-H^+ + $8K^+]^{3-}$, 821.500 (821.518) [◆ + **36**-H^+ + $7K^+]^{4-}$, 649.205 (649.222) [◆ + **36**-H^+ + $6K^+]^{5-}$.

[2,8,9-Trimethyl-2,5,8,9-tetraaza-1-phosphabicyclo[3.3.3]undecane-H^+ ⊂ $Ga_4L_6]^{11-}$ ([37-H^+ ⊂ 1]$^{11-}$): ^1H NMR (500 MHz, D_2O): δ 8.06 (bs, 12H, *aryl*), 7.67 (bs, 12H, *aryl*), 7.21 (d, $J = 8.0$ Hz, 12H, *aryl*), 6.93 (bs, 12H, *aryl*), 6.60 (bs, 12H, *aryl*), 6.48 (bs, 12H, *aryl*). Guest: 0.10 (d, $J = 18.5$ Hz, 9H, N−CH_3), −0.10 to −0.43 (m, 12H, CH_2). $^{31}P\{^1H\}$ (202 MHz, D_2O): δ −14.2 (t, $J = 76$ Hz). TOF MS ES(−) (MeOH), ◆ = $[Ga_4L_6]^{12-}$, calcd (found), *m*/*z*: 1122.354 (1122.364) [◆ + **37**-H^+ + $8K^+]^{3-}$, 832.013 (832.013) [◆ + **37**-H^+ + $7K^+]^{4-}$, 657.826 (657.834) [◆ + **37**-H^+ + $6K^+]^{5-}$.

Acknowledgment. We thank Dr. Dennis Leung, Courtney Hastings, Dr. Shannon Biros, and Dr. Michael Seitz for helpful discussions, Dr. Herman van Halbeek and Rudi Nunlist for assistance with NMR experiments, Dr. Christoph Jocher for help with titrations, and Dr. Ulla Andersen for assistance with mass spectrometry. This work was supported by the Director, Office of Science, Office of Advanced Scientific Computing Research, Office of Basic Energy Sciences (U.S. Department of Energy) under contract DE-AC02-05CH11231 and an NSF predoctoral fellowship to M.D.P.

Supporting Information Available: Eyring plots for the determination of activation parameters of guest self-exchange for **19** and **24**, mass spectrometry data, and raw fits of the SIR data. This material is available free of charge via the Internet at http://pubs.acs.org.

JA072654E